COMPOSITIO MATHEMATICA

Cross-sections of unknotted ribbon disks and algebraic curves

Kyle Hayden

Compositio Math. **155** (2019), 413–423.

doi:10.1112/S0010437X19007012

FOUNDATION
COMPOSITIO
MATHEMATICA

LONDON
MATHEMATICAL
SOCIETY
EST. 1865

Compositio Math. 155 (2019) 413–423
doi:10.1112/S0010437X19007012

Cross-sections of unknotted ribbon disks and algebraic curves

Kyle Hayden

Abstract

We resolve parts (A) and (B) of Problem 1.100 from Kirby's list [*Problems in low-dimensional topology*, in *Geometric topology*, AMS/IP Studies in Advanced Mathematics, vol. 2 (American Mathematical Society, Providence, RI, 1997), 35–473] by showing that many nontrivial links arise as cross-sections of unknotted holomorphic disks in the four-ball. The techniques can be used to produce unknotted ribbon surfaces with prescribed cross-sections, including unknotted Lagrangian disks with nontrivial cross-sections.

1. Introduction

A properly embedded surface Σ in B^4 is said to be *ribbon* if the restriction of the radial distance function from B^4 to Σ is a Morse function with no local maxima. As an important class of examples, holomorphic curves in $B^4 \subset \mathbb{C}^2$ are naturally ribbon. This Morse-theoretic perspective has shed light on the topology of holomorphic curves $\Sigma \subset \mathbb{C}^2$ and the links that arise as transverse intersections $L_r = \Sigma \cap S^3_r$, where S^3_r is a sphere of radius $r > 0$; see [Fie89, BO01, Bor12, Hay17]. Rudolph [Rud83b] and Boileau and Orevkov [BO01] showed that the links obtained as cross-sections of holomorphic curves are precisely the *quasipositive links*, a special class of braid closures. To fully exploit this characterization, it is necessary to understand the relationship between different cross-sections of the same holomorphic curve. This is the subject of Problem 1.100 in Kirby's list.

Problem 1.100A/B [Kir97]. *Let $\Sigma \subset \mathbb{C}^2$ be a smooth algebraic curve, with $L_r = \Sigma \cap S^3_r$ defined as above, and let g denote the Seifert genus.*

(A) *If $r \leqslant R$, is $g(L_r) \leqslant g(L_R)$?*
(B) *If L_R is an unlink and $r \leqslant R$, is L_r an unlink?*

For comparison, by Kronheimer and Mrowka's proof of the local Thom conjecture [KM94], the slice genus g_* is known to satisfy $g_*(L_r) \leqslant g_*(L_R)$ for $r \leqslant R$. In addition, since Seifert and slice genera are equal for strongly quasipositive links by [Rud93], the answer to part (A) of Problem 1.100 is 'yes' when L_r is strongly quasipositive. Part (B) is a special case of part (A), and Gordon's work [Gor81] on ribbon concordance implies that the answer to (B) is 'yes' when L_r is a knot, i.e. connected. In spite of this, we show the answers to (A) and (B) are both 'no'.

Theorem 1. *Every quasipositive slice knot arises as a link component in a cross-section of an unknotted holomorphic disk in $B^4 \subset \mathbb{C}^2$.*

Received 1 March 2018, accepted in final form 8 October 2018, published online 11 February 2019.
2010 Mathematics Subject Classification 57M25 (primary), 32Q55 (secondary).
Keywords: ribbon surfaces, algebraic curves, Lagrangian surfaces, quasipositive links.

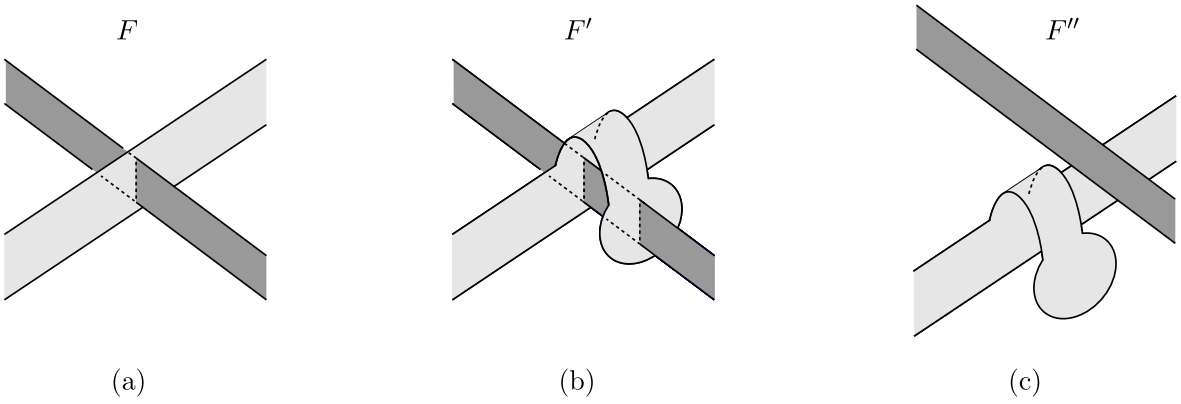

Figure 1. Embedding one ribbon-immersed surface in another, simpler one.

The holomorphic disks constructed in the proof of Theorem 1 are compact pieces of algebraic curves, hence provide the desired counterexamples to part (B) of Problem 1.100. The construction is inspired by a version of the Whitney trick that admits an appealing statement in terms of *ribbon-immersed* surfaces in S^3, i.e. immersed surfaces with boundary whose singularities are of the type depicted in Figure 1(a): *Every ribbon-immersed surface $F \subset S^3$ lies inside a larger one F' that is isotopic (through immersions that are injective along the boundary) to an embedded surface F''*. Moreover, the surface F' may be taken to have the same topological type as F; the construction is depicted in Figure 1. The corresponding four-dimensional construction can be used to embed an arbitrary ribbon surface inside one that is unknotted, i.e. isotopic to an embedded surface in ∂B^4.

Any counterexamples to part (A) of Problem 1.100 constructed using Theorem 1 will have disconnected cross-sections L_r. However, we can use an alternative construction to obtain a sharper result.

Theorem 2. *For every integer $n \geqslant 0$, there is a smooth algebraic curve Σ_n and a pair of positive numbers $r < R$ such that $g(L_r) = 2n+1$ and $g(L_R) = n+1$, where $L_r = \Sigma_n \cap S^3_r$ and $L_R = \Sigma_n \cap S^3_R$ are knots.*

For each Σ_n, the smaller cross-section L_r is a prime quasipositive 4-braid slice knot and L_R is strongly quasipositive.

We also apply these techniques to study Lagrangian cobordisms between Legendrian links, as introduced in [Cha10]. A *Lagrangian filling* of a Legendrian link L in the standard contact S^3 is a properly embedded Lagrangian surface Σ in the standard symplectic B^4 whose boundary is L. We further require the Lagrangian $\Sigma \subset B^4$ to be orientable, exact, and collared; for the significance of these latter two conditions, see [Cha12]. As discussed in [CNS16], it is currently unknown if there are nontrivial knots that arise as collarable cross-sections of a Lagrangian filling of the unknot. We show that the answer is 'yes' if the cross-section is allowed to be disconnected.

Theorem 3. *There are infinitely many nontrivial links that arise as collared cross-sections of unknotted Lagrangian disks in the standard symplectic B^4.*

The remainder of the paper is organized as follows. In § 2, we explain the topological construction underlying our primary results. In § 3, we review the necessary background material

https://doi.org/10.1112/S0010437X19007012 Published online by Cambridge University Press

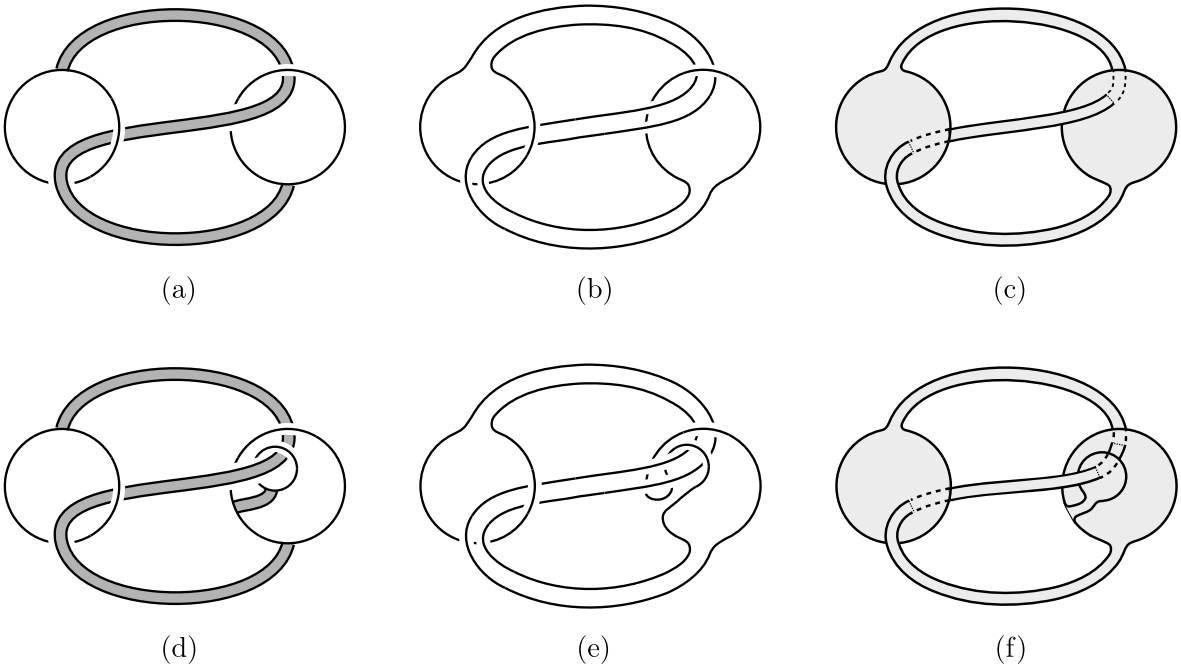

FIGURE 2. Band surgeries on unlinks and the corresponding ribbon surfaces.

on quasipositive braids and then prove Theorems 1 and 2. We close by constructing the Lagrangian disks needed to prove Theorem 3 in § 4.

Remark. In a previous version of this work, it was claimed that Problem 1.100(B) has a positive answer. The argument relied on a statement about unknotted ribbon disks that was shown to be false by Jeffrey Meier and Alexander Zupan in a private correspondence (January 17, 2018). Their illumination of the error in the original argument ultimately led to Theorem 1 above. I wish to thank Meier and Zupan for their invaluable correspondence.

2. The topological construction

This brief section offers an informal account of the topological construction that inspires Theorem 1. Given a link $L \subset S^3$, a *band* $b : I \times I \to S^3$ is an embedding of the unit square such that $L \cap b(I \times I) = b(I \times \partial I)$. A link L' is obtained from L by *band surgery* along b if $L' = (L \backslash b(I \times \partial I)) \cup b(\partial I \times I)$. For example, Figure 2(a, b) presents the stevedore knot 6_1 as the result of band surgery on an unlink. As illustrated in Figure 2(c), a description of a link L as a result of band surgery on an unlink yields a natural ribbon-immersed spanning surface $F \subset S^3$ with $\partial F = L$: simply attach the bands to a collection of embedded disks bounded by the unlink.

In general, a ribbon-immersed surface $F \subset S^3$ will not be isotopic (through immersions that are injective along the boundary) to an embedded surface. However, we can always find another ribbon-immersed surface $F' \subset S^3$ containing F such that F' is isotopic to an embedded surface. The construction is summarized in Figure 1. For an example, see Figure 2(f), where the ribbon disk bounded by the stevedore knot from Figure 2(c) is embedded in a ribbon disk for the unknot that is isotopic to a standard embedded disk.

Under the correspondence between ribbon-immersed surfaces $F \subset S^3$ and ribbon surfaces $\Sigma \subset B^4$ (as in [Has83]), the preceding observation implies that every ribbon disk embeds as a

https://doi.org/10.1112/S0010437X19007012 Published online by Cambridge University Press

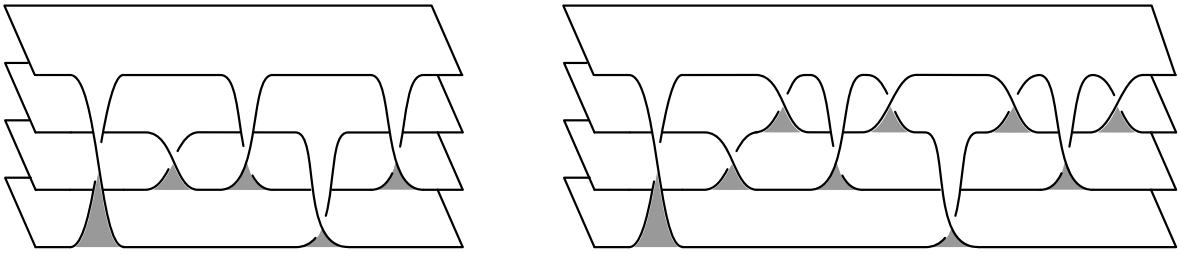

FIGURE 3. Bennequin surfaces for the braids β_0 (left) and β_1 (right).

connected component in a sublevel set of an unknotted ribbon disk. Restricting to the perspective of cross-sections, we obtain a topological version of Theorem 1.

Observation 2.1. Every knot that bounds a ribbon disk in B^4 arises as a link component in a cross-section of an unknotted ribbon disk in B^4.

3. Quasipositive band surgeries and algebraic curves

3.1 Bands and Bennequin surfaces

In [BKL98], Birman, Ko, and Lee define an alternative presentation of the n-stranded braid group B_n using generators of the form

$$\sigma_{i,j} = (\sigma_i \cdots \sigma_{j-2})\sigma_{j-1}(\sigma_i \cdots \sigma_{j-2})^{-1}, \quad 1 \leqslant i \leqslant j \leqslant n.$$

Such generators had been used earlier by Rudolph [Rud83a], who termed $\sigma_{i,j}$ a (positive) *embedded band*. An expression of a braid in B_n as a word w in the generators $\sigma_{i,j}$ is called an *embedded bandword*. Given an embedded bandword w for β, there is a canonical Seifert surface F_w, called the *Bennequin surface*, constructed from n parallel disks by attaching a positively (respectively negatively) twisted embedded band between the ith and jth disks for each term $\sigma_{i,j}$ (respectively $\sigma_{i,j}^{-1}$) in w; see Example 3.1 below. Note that the Euler characteristic of the resulting surface is $n - |w|$, where $|w|$ denotes the length of the embedded bandword.

Example 3.1. The Bennequin surfaces in Figure 3 correspond to embedded bandwords $\beta_0 = \sigma_{1,4}\sigma_2\sigma_{1,3}^{-1}\sigma_{2,4}\sigma_{1,3}$ and $\beta_1 = \sigma_{1,4}\sigma_2\sigma_1\sigma_{1,3}^{-1}\sigma_1^{-1}\sigma_{2,4}\sigma_1\sigma_{1,3}\sigma_1^{-1}$. These are minimal-genus Seifert surfaces for β_0 and β_1. Indeed, we can confirm $g(\beta_0) = 1$ and $g(\beta_1) = 3$ using their Alexander polynomials (which have degree two and six, respectively) and the bound $g(K) \geqslant \deg(\Delta_K)/2$, where K is any knot and $\deg(\Delta_K)$ is defined as the breadth of Δ_K.

A braid is called *strongly quasipositive* if it is a product of positive embedded bands [Rud90], cf. [Rud83a]. More generally, we define a braid to be *quasipositive* if it is a product of arbitrary conjugates of the standard positive generators, i.e. a product of subwords $w\sigma_i w^{-1}$, which we simply call (positive) *bands*. An expression of a braid as a word in these bands is called a *bandword*, and a construction analogous to the one described above associates a ribbon-immersed spanning surface to each bandword.

3.2 Construction of algebraic curves

We now build the desired algebraic curves using a special type of *quasipositive band surgery*: that is, the addition of a band $w\sigma_i w^{-1}$ to a quasipositive braid. This relies on the following lemma, due to Feller [Fel16, Lemma 6].

https://doi.org/10.1112/S0010437X19007012 Published online by Cambridge University Press

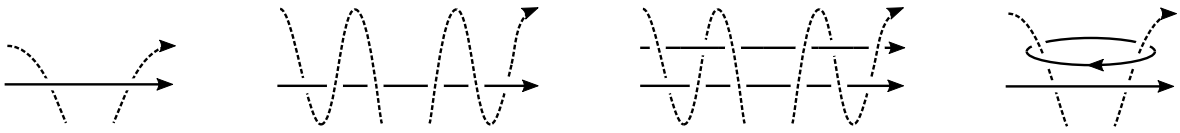

(a) (b) (c) (d)

FIGURE 4. Modifying the original braid (a–c) and its closure (d).

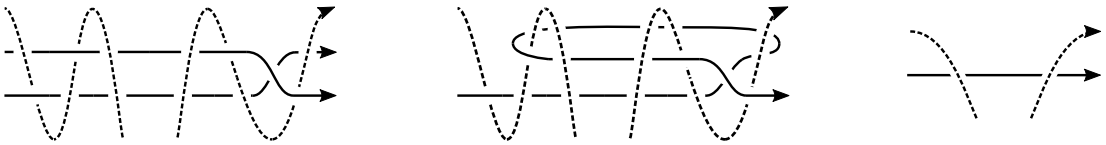

(a) (b) (c)

FIGURE 5. Band surgery and isotopy of the braid closure.

REALIZATION LEMMA (Feller [Fel16], cf. Orevkov [Ore96], Rudolph [Rud83b]). *Let β and γ be quasipositive n-braid words such that γ can be obtained from β by applying a finite number of braid group relations, conjugations, and additions of a conjugate of a positive generator anywhere in the braid. Then there exists a polynomial of the form $p(z,w) = w^n + c_{n-1}(z)w^{n-1} + \cdots + c_0(z)$ and constants $0 < r < R$ such that the intersections of $\Sigma = \{p(z,w) = 0\}$ with S^3_r and S^3_R are isotopic to β and γ, respectively.*

To prove the main theorem, it suffices to adapt the topological construction from § 2 using quasipositive braids and band surgeries.

Proof of Theorem 1. Let $\beta \in B_n$ be a quasipositive braid expressed as a product of positive bands $w\sigma_i w^{-1}$. Let m denote the number of singularities in the ribbon-immersed Bennequin surface F for β. We begin by constructing a quasipositive braid $\beta' \in B_{n+m}$ that contains β as a sublink. Each ribbon singularity in F corresponds to a region in the braid as depicted in Figure 4(a) (or its rotation by 180°, with strand orientations reversed); here the dashed strands represent the crossing strands in the positive band and may pass over or under the black strand in the center of the region where the dashed strands are not drawn. After braid isotopy of the crossing strands, we obtain the quasipositive braid in Figure 4(b). We then introduce an additional strand as shown in Figure 4(c); the new strand passes under all others except at the two points shown in the figure. After performing these modifications for each of the m original singularities, we obtain a quasipositive braid $\beta' \in B_{n+m}$ that contains β as a sublink. Up to smooth isotopy, β' is obtained from β by adding m unknots, linked with β as depicted in Figure 4(d).

Next, let $\gamma \in B_{n+m}$ be the braid obtained from β' by adding a positive generator within each of the m neighborhoods as shown in Figure 5(a). By the lemma, there exists an algebraic curve Σ and constants $0 < r < R$ such that $\beta' = \Sigma \cap \partial B^4_r$ and $\gamma = \Sigma \cap \partial B^4_R$.

Next we show that γ is an unknot. Through the smooth isotopy depicted in Figure 5(b, c), we see that $\gamma \in B_{n+m}$ is isotopic to a quasipositive braid $\gamma' \in B_n$ whose ribbon-immersed Bennequin surface in fact contains no singularities and is therefore embedded. Observe that this braid γ' also has the same number of bands as β. Since the slice-Bennequin inequality is sharp for quasipositive braids [Rud93, Hed10], the number of bands in β equals $n + 2g_*(\beta) - 1 = n - 1$.

https://doi.org/10.1112/S0010437X19007012 Published online by Cambridge University Press

It follows that the Bennequin surface for γ' has Euler characteristic -1, implying that γ' (and thus γ) is an unknot.

Finally, we show that the compact piece of Σ bounded by γ is a holomorphically unknotted disk. For notational convenience, we rescale $\mathbb{C}^2$ so that $R = 1$ and let Σ_1 denote the resulting holomorphic curve in the unit four-ball. That Σ_1 is a disk follows from the fact that holomorphic curves are genus-minimizing [KM94, Rud93]. To show that Σ_1 is holomorphically unknotted, we employ Eliashberg's technique of filling by holomorphic disks (as in [BF98, Proposition 2]). The braid γ can be viewed as a transverse unknot (in the contact-geometric sense) with self-linking number -1. It follows that it bounds an embedded disk $D \subset S^3$ whose characteristic foliation (see [Etn03]) is radial with a single positive elliptic point $p \in D$. There is a small interval $[0, \epsilon)$ and a family of disjoint holomorphic 'Bishop disks' $\Delta_t \subset B^4$ for $t \in [0, \epsilon)$ emerging from p such that Δ_t is properly embedded in B^4 with boundary in $D \subset S^3$ for $t > 0$ (and Δ_0 is a degenerate disk identified with the given elliptic point). By [Eli95, Corollary 2.2B], the Bishop family can be extended to a family of holomorphic disks foliating a three-ball bounded by the piecewise-smooth two-sphere $D \cup \Sigma_1$. In particular, the extended family includes Σ_1, so Σ_1 can be unknotted through holomorphic disks. □

Example 3.2. The quasipositive slice knot given by the mirror of 8_{20} can be represented by the 3-braid $\beta = \sigma_2\sigma_1^2\sigma_2\sigma_1^{-2}\sigma_2^{-1}\sigma_{1,3}$, which embeds in the 5-braid $\beta' = w\sigma_2 w^{-1}\sigma_{1,5}$, where $w = \sigma_4^{-1}\sigma_3^2\sigma_4^{-2}\sigma_3^{-1}\sigma_2^{-1}\sigma_1^2\sigma_2^{-2}\sigma_1^{-1}\sigma_1\sigma_2$. Following the above procedure, β' arises as a cross-section of a holomorphic disk in the four-ball bounded by the unknot $\gamma = w'\sigma_2 w^{-1}\sigma_{1,5}$, where w' is obtained from w by the two replacements $\sigma_3^2 \to \sigma_3\sigma_4\sigma_3$ and $\sigma_1^2 \to \sigma_1\sigma_2\sigma_1$.

Remark 3.3. The construction from the proof above generalizes to show that every quasipositive knot K embeds as a link component in a cross-section of an algebraic curve in the four-ball whose boundary is a strongly quasipositive knot with the same slice genus as K.

Next, we produce the algebraic curves needed for the refined solution to Problem 1.100(A). By [HS00, Theorem 1.6] (see also [ST89]), band surgery decreases the Seifert genus of a knot if and only if the knot has a minimal genus Seifert surface that contains the band. Therefore, to violate the inequality from Problem 1.100(A), we seek pairs of quasipositive braids β and γ such that γ is obtained from β by band surgery along a band lying inside a minimal genus Seifert surface for β.

Proof of Theorem 2. For each $n \geqslant 0$, define a pair of four-braids as follows:

$$\beta_n = \sigma_{1,4}\sigma_2(\sigma_1^n\sigma_{1,3}^{-1}\sigma_1^{-n})\sigma_{2,4}(\sigma_1^n\sigma_{1,3}\sigma_1^{-n}),$$
$$\gamma_n = \sigma_{1,4}\sigma_2\sigma_{2,4}\sigma_1^n\sigma_{1,3}\sigma_2^{n+1}.$$

Observe that each β_n is quasipositive and each γ_n is strongly quasipositive. Bennequin surfaces for β_0 and β_1 appear in Figure 3. We can obtain γ_n from β_n by adding $2n + 2$ positive bands: Adding $\sigma_{1,3}$ in the middle of the term $(\sigma_1^n\sigma_{1,3}^{-1}\sigma_1^{-n})$ in β_n eliminates that entire term, adding σ_1^n to the end of β_n eliminates the term σ_1^{-n}, and then σ_2^{n+1} is added to the end of the word. (The final term is added to ensure that γ_n is a knot and to simplify the expression of its Seifert genus.) By the lemma, there exists an algebraic curve Σ_n and constants $0 < r < R$ such that $\beta_n = \Sigma_n \cap \partial B_r^4$ and $\gamma_n = \Sigma_n \cap \partial B_R^4$.

It remains to calculate the Seifert genera of β_n and γ_n. Since γ_n is strongly quasipositive, its Bennequin surface realizes the Seifert genus of γ_n; see [Rud93]. This surface is built from four

https://doi.org/10.1112/S0010437X19007012 Published online by Cambridge University Press

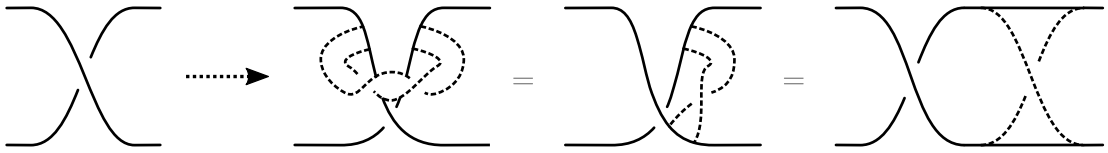

FIGURE 6. Hopf plumbing across a band of like sign.

disks and $5+2n$ bands and has connected boundary, hence has genus $n+1$. To compute the Seifert genus of β_n, we show that its Bennequin surface is also genus-minimizing. This surface is built from four disks and $5+4n$ bands, hence has Euler characteristic $\chi = -1-4n$. Since its boundary is a knot, the genus is $(1-\chi)/2 = 2n+1$. For $n=0$ and $n=1$, we confirmed that these surfaces are genus-minimizing in Example 3.1. We proceed by induction. Let us assume the Bennequin surface for β_{n-1} is minimal, where $n \geqslant 2$. The braid β_n can be viewed as being obtained from β_{n-1} by four replacements of the form $\sigma_1^{\pm 1} \to \sigma_1^{\pm 2}$. As illustrated in Figure 6, the replacement $\sigma_1 \to \sigma_1^2$ can be viewed as the result of plumbing a positive Hopf band across the σ_1-band. The replacement $\sigma_1^{-1} \to \sigma_1^{-2}$ is analogous, realized by plumbing a negative Hopf band across a σ_1^{-1}-band. It follows that the Bennequin surface for β_n is obtained from that of β_{n-1} by repeated Hopf plumbing. Since the Bennequin surface for β_{n-1} is genus-minimizing, it follows from [Gab83] that the Bennequin surface for β_n is genus-minimizing as well. □

4. Unknotted Lagrangian disks with nontrivial cross-sections

In this final section, we adapt the construction from § 2 to the Lagrangian setting. We assume the reader is familiar with the basics of Legendrian knot theory and front diagrams for Legendrian links; see, for example, Etnyre's survey [Etn05]. For background on Lagrangian fillings of Legendrian links, see [Cha10].

We use the following theorem to construct the desired Lagrangian surfaces.

THEOREM 4.1 [BST15, Cha10, EHK16, Dim16]. *If two Legendrian links $L_\pm$ in the standard contact S^3 are related by any of the following three moves, then there exists an exact, embedded, orientable, and collared Lagrangian cobordism from L_- to L_+.*

Isotopy: *L_- and L_+ are Legendrian isotopic.*

0-Handle: *The front of L_+ is the same as that of L_- except for the addition of a disjoint Legendrian unknot as in the left side of Figure 7.*

1-Handle: *The fronts of $L_\pm$ are related as in the right side of Figure 7.*

Remark 4.2. A cross-section $\Sigma \cap S^3_r$ of a Lagrangian surface $\Sigma \subset B^4$ is said to be *collarable* if there exists $\epsilon > 0$ and a family of isotopic Lagrangian surfaces Σ_t with $\Sigma_0 = \Sigma$ such that: (i) for all $t \in [0,1]$, Σ_t is transverse to S^3_r and coincides with Σ outside $B^4_{r+\epsilon} \setminus \operatorname{int}(B^4_{r-\epsilon})$; (ii) the vector field $\partial/\partial r$ is tangent to Σ_1 near the cross-section $S^3_r \cap \Sigma_1$.

FIGURE 7. Diagram moves corresponding to attaching a 0-handle and an oriented 1-handle.

https://doi.org/10.1112/S0010437X19007012 Published online by Cambridge University Press

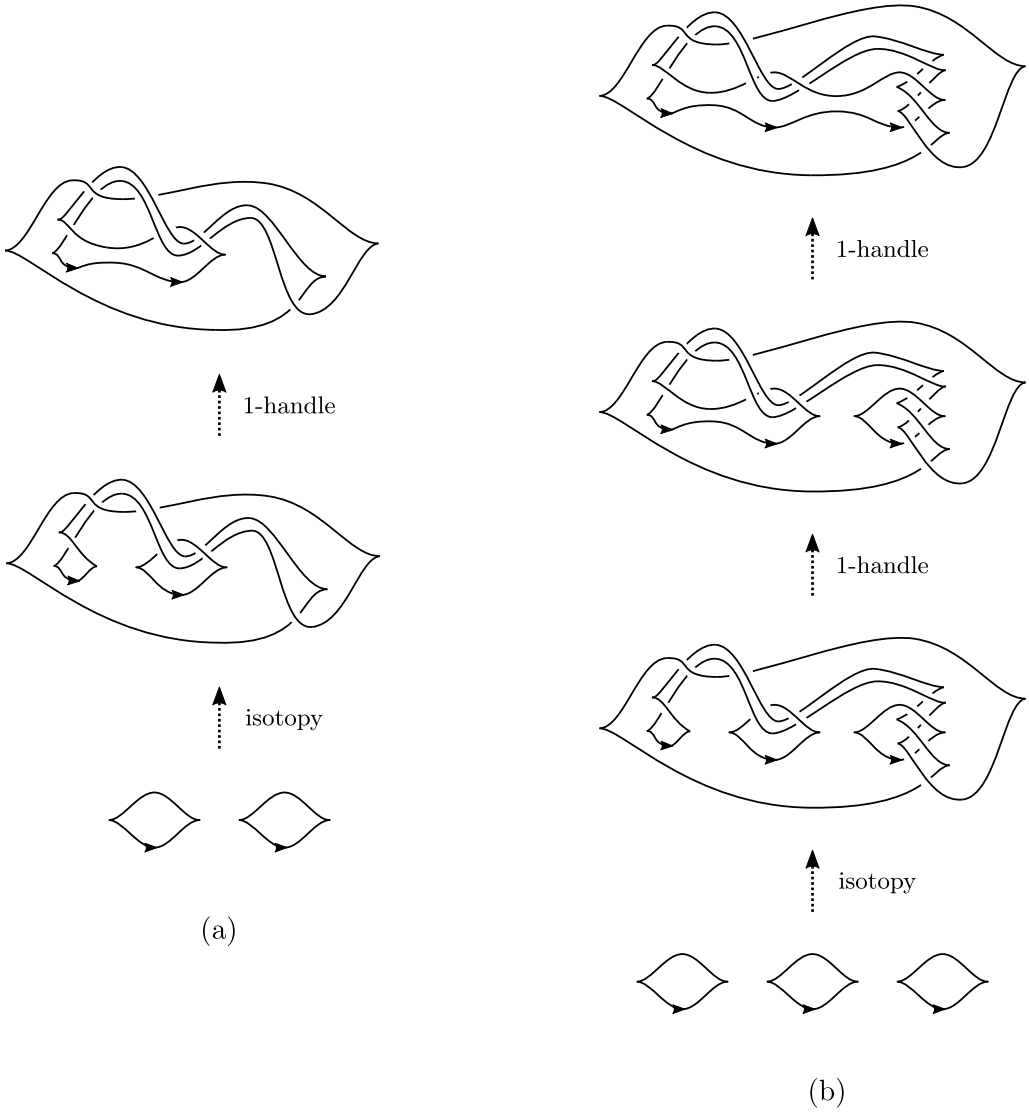

Figure 8. A pair of Lagrangian disks.

Example 4.3. Consider the sequences of front diagrams in Figure 8. The implied first step in each sequence is the attachment of some number of 0-handles. Applying Theorem 4.1, part (a) corresponds to a Lagrangian filling of the mirror of the knot 9_{46}, which is seen to be a disk because it consists of two 0-handles joined by a single 1-handle. (This sequence is adapted from [HS15, Example 4.1].) Part (b) corresponds to a Lagrangian disk bounded by a Legendrian unknot. Observe that the penultimate front in this sequence depicts a two-component link formed from the knot $11n_{139}$ and an unknot.

To prove Theorem 3, we generalize the construction from part (b) of Figure 8.

Proof of Theorem 3. Let K be a Legendrian knot that bounds a ribbon-immersed disk in S^3 whose n ribbon singularities all have the special form depicted on the left side of Figure 9. Moreover, let us assume that the link L obtained by resolving each such singularity as in Figure 9

https://doi.org/10.1112/S0010437X19007012 Published online by Cambridge University Press

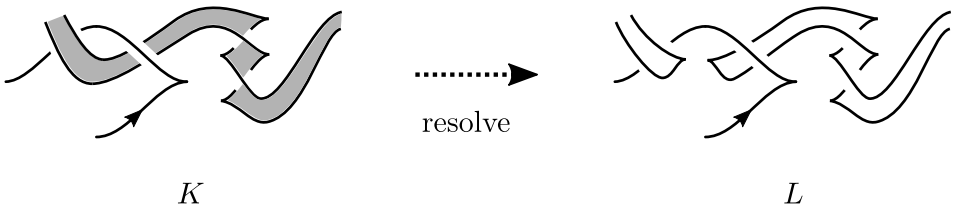

FIGURE 9. Resolving a ribbon singularity.

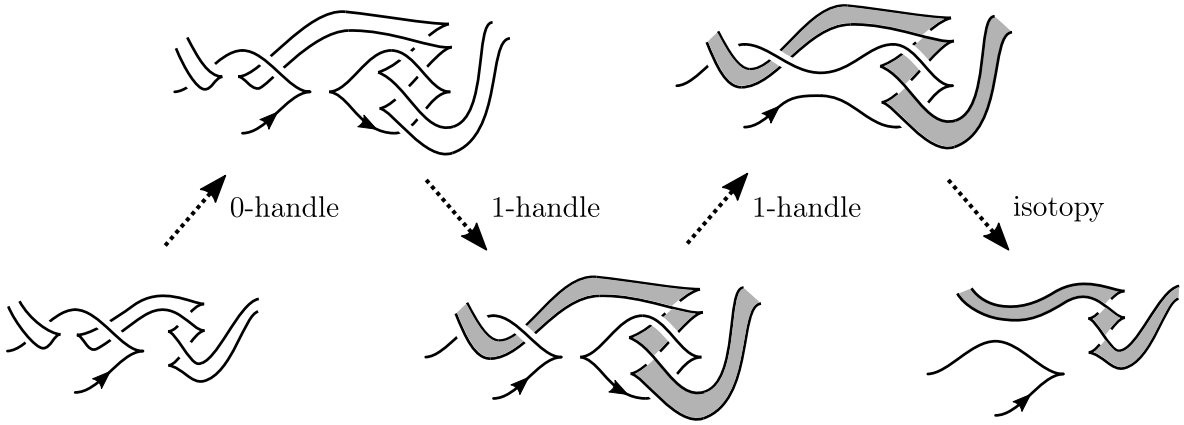

FIGURE 10. Constructing an unknotted Lagrangian disk with a nontrivial cross-section.

is an $(n+1)$-component unlink, each of whose components bounds a Lagrangian disk constructed as in Theorem 4.1. Working in reverse, we can attach 1-handles to this collection of disks to obtain a single Lagrangian disk Σ bounded by K. As discussed in Remark 4.4 below, one can readily produce infinitely many knots that fit into this construction.

We claim that Σ embeds into an unknotted Lagrangian disk Σ'. To see this, consider the $(2n+1)$-component unlink L' obtained from L by introducing unknotted components near each ribbon singularity as in the first step of Figure 10. This unlink bounds a collection of $(2n+1)$ Lagrangian disks. By attaching n 1-handles as in the second step of Figure 10, we obtain a collection of $(n+1)$ Lagrangian disks; this collection consists of Σ linked with n unknotted disks. Finally, we attach n more 1-handles as shown in the third step of Figure 10, producing a single Lagrangian disk Σ'. All ribbon singularities of the corresponding ribbon-immersed surface in S^3 can be eliminated using the isotopy in the final step of Figure 10, so the boundary of Σ' is an unknot. By construction, Σ' contains K as a link component in a collared cross-section.

To see that these Lagrangian fillings of the unknot are unknotted as embedded disks in B^4, we appeal to work of Eliashberg and Polterovich [EP96] which implies that any two properly embedded Lagrangian disks in B^4 with collared, unknotted boundary are in fact isotopic through such Lagrangian disks. Therefore, the fillings of the unknot constructed above are isotopic to the standard unknotted filling of the unknot. □

Remark 4.4. To produce examples of Legendrian knots fitting into the above construction, it can be convenient to start with a Legendrian knot K' that can be transformed into a Lagrangian-fillable unlink by applying resolutions of the form depicted in Figure 11. By modifying each of

https://doi.org/10.1112/S0010437X19007012 Published online by Cambridge University Press

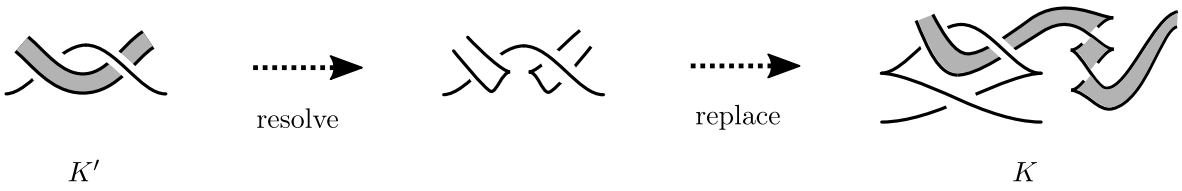

Figure 11. Producing knots that fit into the construction from the proof of Theorem 3.

these regions as shown, we obtain a Legendrian knot K which also bounds a Lagrangian disk and fits into the construction from the proof of Theorem 3.

Acknowledgements

I wish to thank Lee Rudolph for bringing these questions to my attention and Eli Grigsby for numerous stimulating conversations about braids and ribbon surfaces. Thanks also to Peter Feller, Patrick Orson, and the anonymous referee for comments on drafts, and to Siddhi Krishna, Clayton McDonald, Jeffrey Meier, and Alexander Zupan for helpful conversations.

References

BKL98 J. Birman, K. H. Ko and S. J. Lee, *A new approach to the word and conjugacy problems in the braid groups*, Adv. Math. **139** (1998), 322–353.

BF98 M. Boileau and L. Fourrier, *Knot theory and plane algebraic curves*, Chaos Solitons Fractals **9** (1998), 779–792.

BO01 M. Boileau and S. Orevkov, *Quasi-positivité d'une courbe analytique dans une boule pseudo-convexe*, C. R. Acad. Sci. Paris Sér. I Math. **332** (2001), 825–830.

Bor12 M. Borodzik, *Morse theory for plane algebraic curves*, J. Topol. **5** (2012), 341–365.

BST15 F. Bourgeois, J. M. Sabloff and L. Traynor, *Lagrangian cobordisms via generating families: construction and geography*, Algebr. Geom. Topol. **15** (2015), 2439–2477.

Cha10 B. Chantraine, *On Lagrangian concordance of Legendrian knots*, Algebr. Geom. Topol. **10** (2010), 63–85.

Cha12 B. Chantraine, *Some non-collarable slices of Lagrangian surfaces*, Bull. Lond. Math. Soc. **44** (2012), 981–987.

CNS16 C. Cornwell, L. Ng and S. Sivek, *Obstructions to Lagrangian concordance*, Algebr. Geom. Topol. **16** (2016), 797–824.

Dim16 G. Dimitroglou Rizell, *Legendrian ambient surgery and Legendrian contact homology*, J. Symplectic Geom. **14** (2016), 811–901.

EHK16 T. Ekholm, K. Honda and T. Kálmán, *Legendrian knots and exact Lagrangian cobordisms*, J. Eur. Math. Soc. (JEMS) **18** (2016), 2627–2689.

Eli95 Ya. Eliashberg, *Topology of 2-knots in* $\mathbf{R}^4$ *and symplectic geometry*, in *The Floer memorial volume*, Progress in Mathematics, vol. 133 (Birkhäuser, Basel, 1995), 335–353.

EP96 Ya. Eliashberg and L. Polterovich, *Local Lagrangian 2-knots are trivial*, Ann. of Math. (2) **144** (1996), 61–76.

Etn03 J. B. Etnyre, *Introductory lectures on contact geometry*, in *Topology and geometry of manifolds, Athens, GA, 2001*, Proceedings of Symposia in Pure Mathematics, vol. 71 (American Mathematical Society, Providence, RI, 2003), 81–107.

Etn05 J. Etnyre, *Legendrian and transversal knots*, in *Handbook of knot theory* (Elsevier, Amsterdam, 2005), 105–185.

Fel16 P. Feller, *Optimal cobordisms between torus knots*, Comm. Anal. Geom. **24** (2016), 993–1025.

Fie89 T. Fiedler, *Complex plane curves in the ball*, Invent. Math. **95** (1989), 479–506.

Gab83 D. Gabai, *The Murasugi sum is a natural geometric operation*, in *Low-dimensional topology, San Francisco, CA, 1981*, Contemporary Mathematics, vol. 20 (American Mathematical Society, Providence, RI, 1983), 131–143.

Gor81 C. McA. Gordon, *Ribbon concordance of knots in the 3-sphere*, Math. Ann. **257** (1981), 157–170.

Has83 J. Hass, *The geometry of the slice-ribbon problem*, Math. Proc. Cambridge Philos. Soc. **94** (1983), 101–108.

Hay17 K. Hayden, *Quasipositive links and Stein surfaces*, Preprint (2017), arXiv:1703.10150.

HS15 K. Hayden and J. M. Sabloff, *Positive knots and Lagrangian fillability*, Proc. Amer. Math. Soc. **143** (2015), 1813–1821.

Hed10 M. Hedden, *Notions of positivity and the Ozsváth–Szabó concordance invariant*, J. Knot Theory Ramifications **19** (2010), 617–629.

HS00 M. Hirasawa and K. Shimokawa, *Dehn surgeries on strongly invertible knots which yield lens spaces*, Proc. Amer. Math. Soc. **128** (2000), 3445–3451.

Kir97 R. Kirby, *Problems in low-dimensional topology*, in *Geometric topology*, AMS/IP Studies in Advanced Mathematics, vol. 2, ed. W. H. Kazez (American Mathematical Society, Providence, RI, 1997), 35–473.

KM94 P. B. Kronheimer and T. S. Mrowka, *The genus of embedded surfaces in the projective plane*, Math. Res. Lett. **1** (1994), 797–808.

Ore96 S. Yu. Orevkov, *Rudolph diagrams and analytic realization of the Vitushkin covering*, Mat. Zametki **60** (1996), 206–224, 319.

Rud83a L. Rudolph, *Braided surfaces and Seifert ribbons for closed braids*, Comment. Math. Helv. **58** (1983), 1–37.

Rud83b L. Rudolph, *Algebraic functions and closed braids*, Topology **22** (1983), 191–202.

Rud90 L. Rudolph, *A congruence between link polynomials*, Math. Proc. Cambridge Philos. Soc. **107** (1990), 319–327.

Rud93 L. Rudolph, *Quasipositivity as an obstruction to sliceness*, Bull. Amer. Math. Soc. (N.S.) **29** (1993), 51–59.

ST89 M. Scharlemann and A. Thompson, *Link genus and the Conway moves*, Comment. Math. Helv. **64** (1989), 527–535.

Kyle Hayden hayden@math.columbia.edu
Department of Mathematics, Columbia University,
New York, NY 10027, USA

https://doi.org/10.1112/S0010437X19007012 Published online by Cambridge University Press